Experiments on the Onset of Water Accumulation and CCFL Through a Multi-hole Plate in a Vertical Tank

Kyung-Won Lee and Hee Cheon NO

Korea Advanced Institute of Science and Technology
373-1, Guseong-dong, Yuseong-gu, Daejeon, 305-701, Korea

Chul-Hwa SONG

Korea Atomic Energy Research Institute
150, Dukjin-dong, Yuseong-gu, Daejeon, 305-353, Korea

Abstract

An experimental study was performed to investigate the air-water countercurrent flow limitation through perforated plates inside a vertical tube. Effects of plate thicknesses, multiple holes and the location of air vent line on the onset of water accumulation or on the onset of countercurrent flow limitation were examined. In addition, the influence of the location of air vent line on water level distributions was investigated. A new Kutateladze type correlation for the onset of water accumulation was developed and present experimental results were compared with existing correlations and data.

1. Introduction

During the reflood phase of a large break loss of coolant accident (LBLOCA) in a PWR, steam-water countercurrent flow can occur between the steam flow from the core region and the water de-entrained in the upper plenum. Since the occurrence of countercurrent flow limitation (CCFL) in the upper core support plate (UCSP), end box, and tie plate have considerable influence on the effectiveness of the emergency core cooling [1], it is very

important to investigate the factors affecting the onsets of water accumulation and countercurrent flow limitation (CCFL).

Although numerous studies on the gas-liquid mixing and CCFL in perforated plates have already been conducted extensively ([2]-[6]), there are no available experimental data that are applicable to plates with large hole diameters like UCSP.　Test section geometries and main objectives used in previous experiments are summarized in Table 1.

The main purposes of the present study are to evaluate the parametric effects of plate thickness, multiple large holes, and air vent line locations on the onsets of water accumulation, CCFL, and water level distributions.

2. Experiments

2.1 Experimental Apparatus

A schematic diagram of the experimental apparatus is shown Fig. 1.　The main components of the system are (1) test section, (2) the water supply system, (3) the air supply system, and (4) the data acquisition system.

In the present study, the perforated plate with 4 or 12 holes (same diameter of 0.05m and pitch of 0.096m) is installed at the middle height of the vessel (a height of 2m and inner diameter of 0.48m) to simulate the UCSP and the upper plenum of a PWR.　Plate geometries used in the present test are shown in Fig. 2.

Flow conditions in the upper plenum during the reflood phase of LBLOCAs are simulated using air and water.　The water was supplied from the water storage tank maintained constant head and injected into the upper plenum through four water injection lines.　A concentric barrier was installed in the vessel.　Thus, the injected water into the upper plenum bumped into this barrier, spread widely, and consequently, flowed downward. The water flow rate was measured by the rotameter.

Air, which was supplied by an air blower, was injected into the lower plenum through two air injection lines and passed through the plate holes, the upper plenum and the air vent line. The air flow rate was measured by the vortex flow meter.

2.2 Test Parameters and Test Procedure

The controllable test parameters were the flow rates of air and water, the number of plate holes, the plate thickness, and the location of air vent line.　In the present experiment, the

water flow rate was held constant while the air flow rate was increased step by step. The onsets of water accumulation and CCFL were determined by the change in collapsed water level on the plate. The two-phase mixture level on the plate is evaluated by the visual observation and the collapsed water level is determined by measuring the change in the pressure difference between the bottom and the top of the upper plenum.

3. Data Analysis

The most widely used flooding (or CCFL) correlation is the Wallis type correlation and the Kutatetladze type correlation expressed as

$$j_g^{*\ 1/2} + m_w\ j_f^{*\ 1/2} = C_w \tag{Eq. 1}$$

$$K_g^{1/2} + m_k\ K_f^{1/2} = C_w \tag{Eq. 2}$$

where m and C are empirically determined constants. The parameters, j_k^* and K_k , are the dimensionless superficial velocity and the Kutateladze number of each phase k (f denotes liquid phase and g denotes gas phase), respectively and expressed as

$$j_k^* = j_k \left[\frac{\rho_k}{gD(\rho_f - \rho_g)} \right]^{1/2} \tag{Eq. 3}$$

$$K_k = j_k \left[\frac{\rho_k^{\ 2}}{g\sigma(\rho_f - \rho_g)} \right]^{1/4} \tag{Eq. 4}$$

In the above equations, j_k and ρ_k are the superficial velocity and the density of each phase of k, and D and σ are the tube diameter and the surface tension.

Celata et al. [2] proposed a Wallis type correlation for the CCFL with

$$m_w = 1, \quad C_w = \gamma^{0.35} \tag{Eq. 5}$$

For perforated plates, Bankoff et al. [3] suggested a correlation using the dimensionless parameter H_k^* expressed as

$$H_g^{*\ 1/2} + H_f^{*\ 1/2} = C_b \tag{Eq. 6}$$

where H_k^* is the dimensionless flux of each phase of k and has the form

$$H_k^* = j_k \left[\frac{\rho_k}{gw(\rho_f - \rho_g)} \right]^{1/2} \qquad \text{(Eq. 7)}$$

where w is the interpolative length scale given by

$$w = D^{1-\beta} \left[\frac{\sigma}{g(\rho_f - \rho_g)} \right]^{\beta/2} \quad (0 \le \beta \le 1) \qquad \text{(Eq. 8)}$$

$$\beta = \tanh(\gamma \, k_c D) \qquad \text{(Eq. 9)}$$

$$k_c = 2\pi / t_p \qquad \text{(Eq. 10)}$$

where k_c is the critical wave number and t_p is the plate thickness.

Equations 7 and 9 imply that the parameter H_k^* approaches j_k^* for small hole diameters, small perforation ratios, and large plate thicknesses, while it approaches K_k for large hole diameters, large perforation ratios and thin plates.

The parameter C is a function only of geometry and reflects entrance and exit effects, Bankoff et al. [3] suggested C of the form

$$C_b = 1.07 + 4.33 \times 10^{-3} L^* \quad (L^* < 200)$$
$$C_b = 2 \qquad\qquad\qquad\quad (L^* > 200) \qquad \text{(Eq. 11)}$$

where L^* is a Bond number defined as

$$L^* = n\pi D \left[\frac{g(\rho_f - \rho_g)}{\sigma} \right]^{1/2} \qquad \text{(Eq. 12)}$$

and n is the number of holes.

4. Results and Discussion

4.1 Definition of Onsets of Water Accumulation and CCFL

Figure 3 shows the definition of onsets of water accumulation and CCFL. In this study, the air flow rate was increased step by step for given water flow rate (10 lpm) as shown in Fig. 3. At the very low air flow rate, air and water flow countercurrently in the form of the separated flow without large disturbances (region A). But, as the air flow rate increased, air-water mixing occurred at plate holes suddenly. Consequently, air-water two-phase mixture

level began to increase dramatically. This point was defined as the onset of water accumulation in this study. Liu et al. [4] and Lee et al. [5] used terms like 'onset of flooding' or 'onset of mixing' to represent the change of the flow configuration from separate to mixing flow (onset of water accumulation) at the plate holes.

After the onset of water accumulation, both the air-water mixture level and the collapsed water level remain constant but increase with an increase in the air flow rate (region B). The constant collapsed water means that all the water flow rate injected into the upper plenum flows downward, that is, there is no real limitation of water downward flow.

As the air flow rate is further increased to a sufficiently high flow rate, the collapsed water level increases continuously in spite of the constant air flow rate (region C).   In this region, the water penetration rate through the plate is smaller than the injected water flow rate and this point is defined as the onset of CCFL. Zhang et al. [6] used the term of 'onset of flooding' to represent the point at which the superficial liquid penetration velocity begins to decrease (onset of CCFL in this study) and used the term of CCFL to represent the liquid zero penetration.

4.2 Effects of Number of Holes and the Plate Thickness on the Onset of Water Accumulation

The effect of the number of plate holes was investigated by comparing the results between 4-hole plate (perforation ratio, $\gamma = 4.3\%$) and 12-hole plate ($\gamma = 13\%$).   In addition, the effect of the plate thickness on the onset of water accumulation was also examined by comparing the results between 1cm-plate and 4cm-plate.   In the present study, *d, t, n, and p* denote the hole diameter, the plate thickness, the number of holes, and the pitch between holes, respectively.

In Fig. 4, some present experimental data for the onset of water accumulation were plotted in the form of Kutateladze numbers.   Since there was no difference between the injected water flow rate and the downward water penetration rate before the onset of CCFL, water Kutateladze numbers were calculated from the inlet water flow rates.

Results show that the onset of water accumulation is promoted as the number of holes decrease, while the plate thickness has a negligible effect on the onset of water accumulation. In case the number of holes is reduced, the water downward flow can be strongly affected by the uprising air flow because the air and water must go through a small number of holes. Therefore, the onset of water accumulation can occur at the lower air flow rate per hole. But, this result is incompatible with Liu's experimental data.   Liu et al. [4] reported that the

onset of water accumulation was promoted by a larger number of paths though the influence appeared to be weak.   They suggested that the surface waves generated from the 'early-flooded' holes by the initial uneven water distribution were responsible for inducing the remaining holes to flood.

4.3 Effect of the Location of Air Vent Line on the Onset of Water Accumulation

In order to investigate the effect of asymmetric air flow on the onset of water accumulation in the upper plenum, a hot-leg (inner diameter = 10cm) was installed at the middle height of the upper plenum (50cm distance from the UCSP).   In case the hot-leg was installed, the air vent line located at the top of the upper plenum was closed completely, and so air was vented only through the hot-leg.   From the results shown in Fig. 5, it is obvious that the location of the air vent line in the upper plenum does not affect the gas flow rate required for the onset of water accumulation.   In Fig.5, the term 'without hot-leg' means that the top air vent line is used.   A small amount of water carry-over out of the test vessel occurred when the hot-leg was installed, but those amounts were at most 0.9% in comparison with the injected water flow rate.   Thus, carry-over rates were ignored in calculating the water Kutateladze numbers.

4.4 Effect of the Location of Air Vent Line on the Distribution of Collapsed Water Level

Figure 6 shows the effect of asymmetric air flow on the distribution of collapsed water level on the 12- hole plate with 4cm-thickness.   To investigate the level distribution, collapsed water levels were measured at different two points, namely, Level 1 and Level 2 as shown in Fig. 2 and the distance between two points was 19.2cm.
The results shows that collapsed water levels increase with the flow rates of air or water. But, there is no change in collapsed water levels between two points in spite of the asymmetric air flow in the upper plenum.   The collapsed water levels remain constant at a relatively low water flow rate, while those are highly agitated at high water flow rate.

4.5 Development of an Empirical Correlation for the Onset of Water Accumulation

Based on the present experimental data, a new Kutateladze type correlation for the onset of water accumulation was developed using a least-square fit method as follows:

$$K_g^{1/2} + 1.17 \, K_f^{1/2} = 1.36 \qquad\qquad\qquad \text{(Eq. 13)}$$

Eq. 13 can be applicable to the present plate conditions as shown in Table. 1.

The present experimental data were also compared with Liu's data [4]. As can be seen in Fig. 7, the onsets of water accumulation occur at slightly higher air flow rates in the present experiment. However, it is difficult to quantify the reasons for this because there are large differences in experimental conditions such as the hole diameter, the number of holes and the distance between holes.

4.6 Effect of the Plate Thickness on Onsets of Water Accumulation and CCFL

Figures 8 through 10 show the effect of plate thickness on the onset of CCFL at the 4-hole plate. For given water flow rate, the onset of CCFL occurred at the nearly same air flow rate regardless of the plate thickness (1cm-thickness and 4cm-thickness). Thus, when the present data were expressed with the dimensionless superficial velocity or the Kutateladze number, the results were nearly the same for two kinds of plate thicknesses as shown in Figs. 8 and 9. In Fig. 8, it is evident that Celata's correlation [2] is not applicable to the very low perforation ratios.

The present CCFL data were also compared with Bankoff's correlation [2] and Zhang's CCFL data [6] in Fig. 10. The result shows that there is a large difference between the present data and the Bankoff's correlation. The reasons for this difference may be due to the followings. Firstly, the dimensionless volumetric flux, H_k^* , includes the information of plate thickness. Secondly, there is an appreciable difference in experimental conditions such as perforation ratios and plate hole diameters.

5. Conclusions

An experimental study was performed to investigate the air-water countercurrent flow limitation through perforated plates in the vertical tube. The main conclusions of the present work can be summarized as follows:

(1) The onset of water accumulation is promoted as the number of holes decreases, while the plate thickness has a negligible effect on the onset of water accumulation.
(2) In the present experiment, the location of the air vent line in the upper plenum does not

affect the onset of water accumulation and the collapsed water level distribution.

(3) Based on the present experimental data, a new Kutateladze type correlation for the onset of water accumulation was developed.

(4) For given water flow rate, the onset of CCFL occurs at the nearly same air flow rate regardless of the plate thickness.

References

[1] Damerell, P. S. and Simons, J. W., Reactor safety issues resolved by the 2D/3D program, NUREG/IA-0127, 1993.

[2] Celata, G. P., Cumo, N., Farello, G. E., and Setaro, T., "The influence of flow obstructions on the flooding phenomenon in vertical channels," Int. J. Multiphase Flow, vol.15, No.2, pp.227-239, 1989.

[3] Bankoff, S.G., Takin, R. S., Yuen, M. C., and Hsieh, C. L., "Countercurrent flow of air/water and steam/water through a horizontal perforated plate," Int. J. Heat and Mass Transfer, vol.24, No.8, pp.1381-1395, 1981.

[4] Liu, C. P., McCarthy, G. E., and Tien, C. L., "Flooding in vertical gas-liquid countercurrent flow through multiple short paths," Int. J. Heat and Mass Transfer, vol.25, No.9, pp.1301-1312, 1982.

[5] Lee H. M., McCarthy G. E., and Tien C. L., "Liquid carry-over and Entrainment in Air-Water Countercurrent Flooding," EPRI NP-2344, 1982.

[6] Zhang, J., Seynhaeve, J. M., and Giot, M., "Experiments on the hydrodynamics of air-water countercurrent flow through vertical short multitube geometries," Experimental Thermal and Fluid Science, vol.5, pp. 755-769, 1992.

[7] Glaeser, H., "Downcomer and tie plate countercurrent flow in the upper plenum test facility (UPTF)," Nuclear Engineering and Design, vol.133, pp.259-283, 1992.

Table 1 Test section geometries and main objectives of previous experiments

	Test Section Geometries						Main Objectives
	Tube Diameter (cm)	Plate Thickness (cm)	Plate Hole Diameter (cm)	No. of Holes	Pitch (cm)	Perforation Ratio (%)	
Liu et al. (1982)	14.6	1.27 plate, stub	1.27, 1.905	1, 2, 3, 7	0 ~ 4.7 (5cases)	1.7 ~ 11.9 (5 cases)	Onset of water accumulation
Lee et al. (1982)	10.08	1.27	2.57 ~ 7.62 (5 cases)	1, 2, 3	-	19.4 ~ 57.1 (3 cases)	Onset of liquid carry-over
Bankoff et al. (1982)	7.15×4.29 rectangular channel	2.0	0.48, 1.05, 2.86	2, 3, 5, 9,15,40	< 3.58 (5 cases)	8.47 ~ 42.34 (6 cases)	CCFL
Celata et al. (1989)	1.62, 2	0.12 ~ 0.2	0.7 ~ 1.9 (9 cases)	1, 4	-	36 ~ 100 (8 cases)	CCFL
Zhang et al. (1992)	10	7.2, 36, 72	3.6	3	11.6	38.9	CCFL
Present Experiment (2004)	48	1, 4	5	4, 12	9.6	4.3, 13	Onset of water accumulation, Level distribution
	48	1, 4	5	4	9.6	4.3	Onset of CCFL
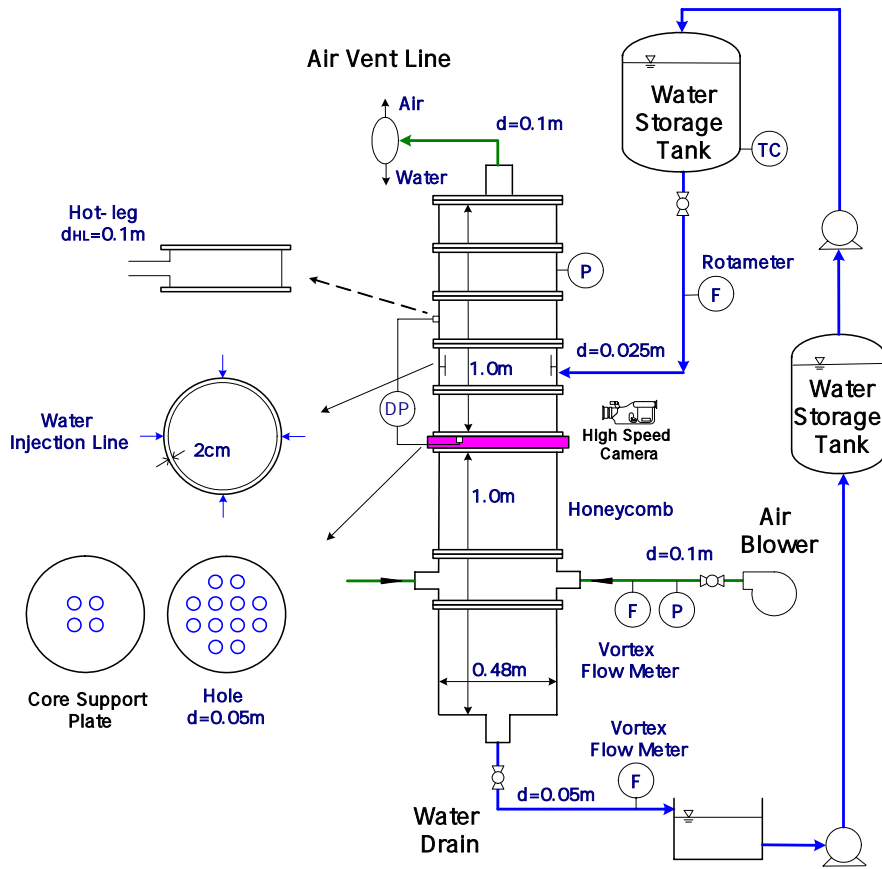
Fig. 1 Schematic diagram of experimental apparatus
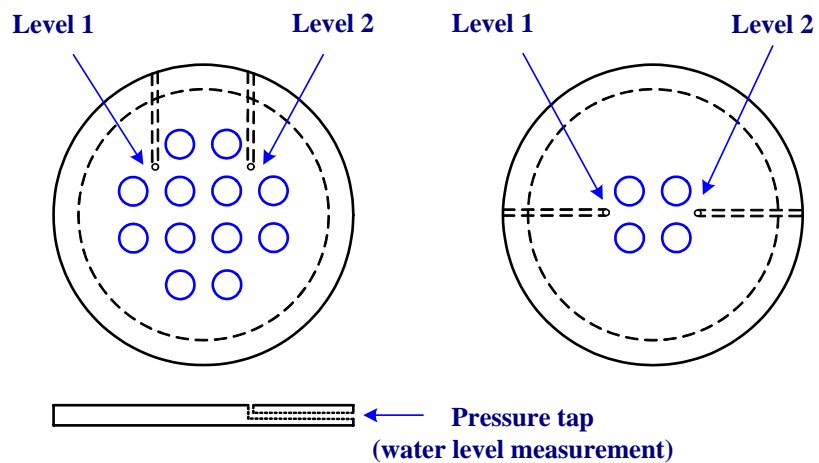
Fig. 2 Plate geometries
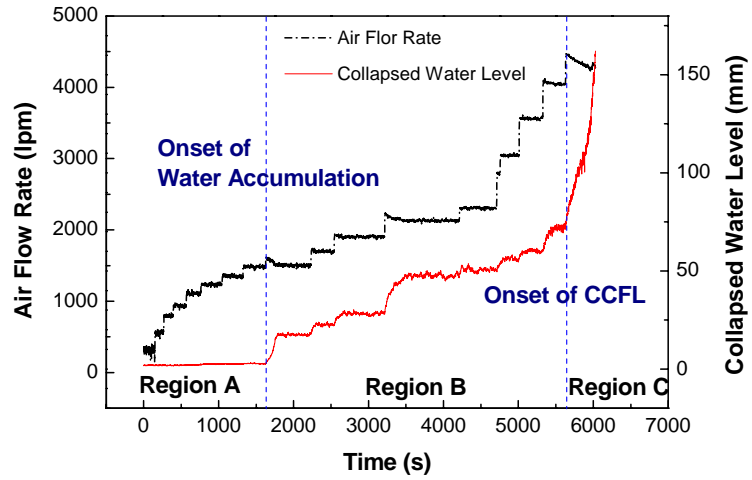
Fig. 3 Definition of onsets of water accumulation and CCFL
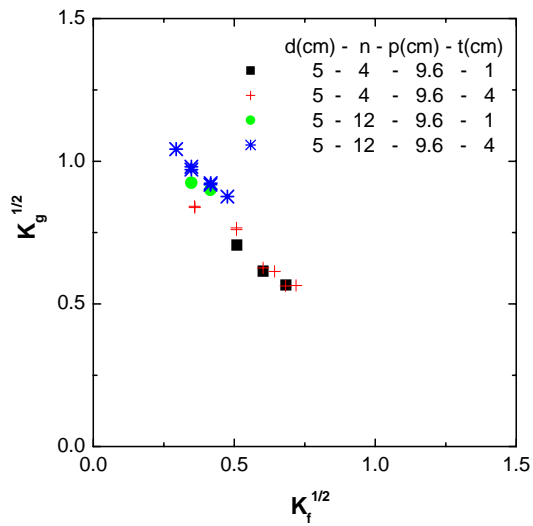
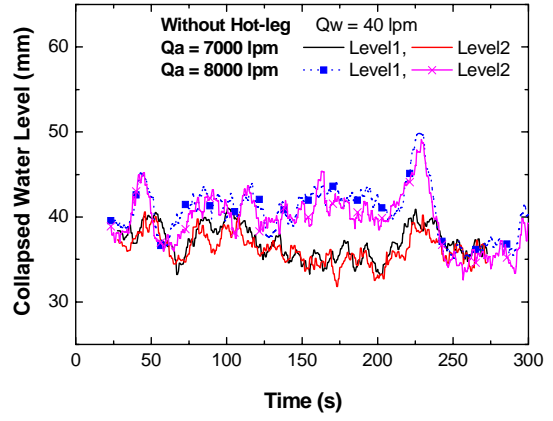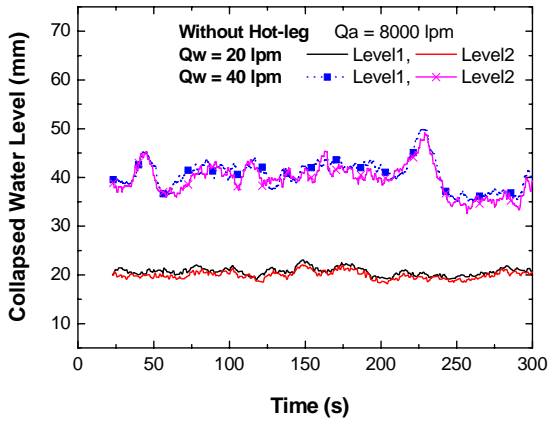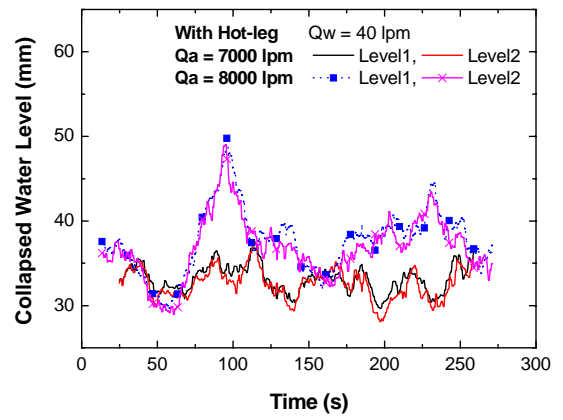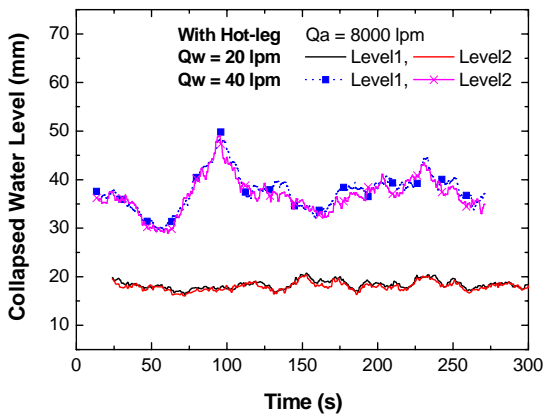Fig. 4 Effects of the number of holes and plate thickness
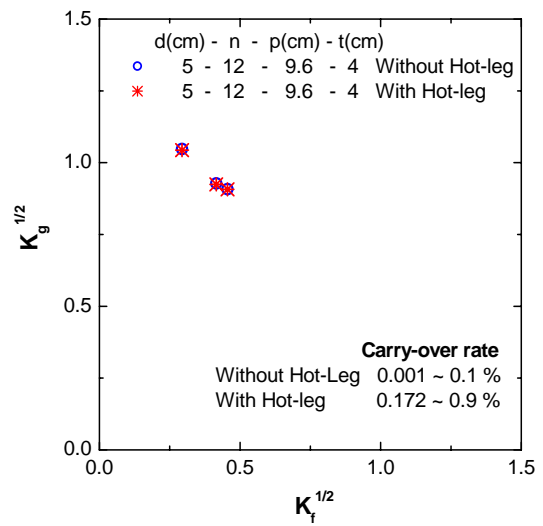
Fig. 5 Effects of the location of air vent line

(a) Collapsed water level distributions without hot-leg

(b) Collapsed water level distributions with hot-leg

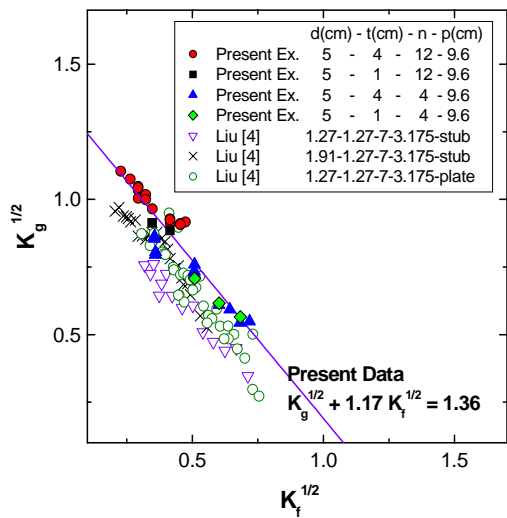Fig. 6 Collapsed water level distributions with and without hot-leg

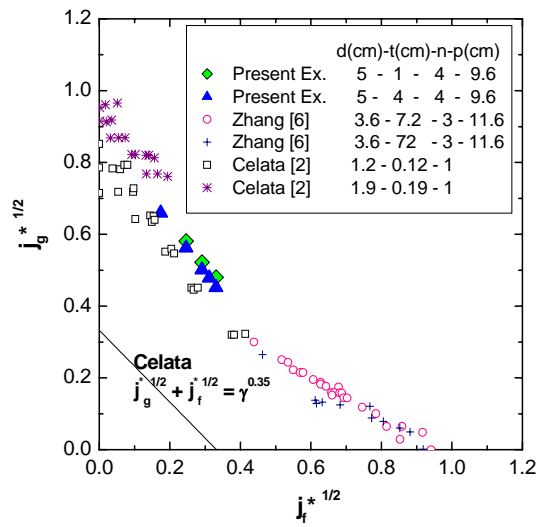Fig. 7 Present data for the onset of water accumulation

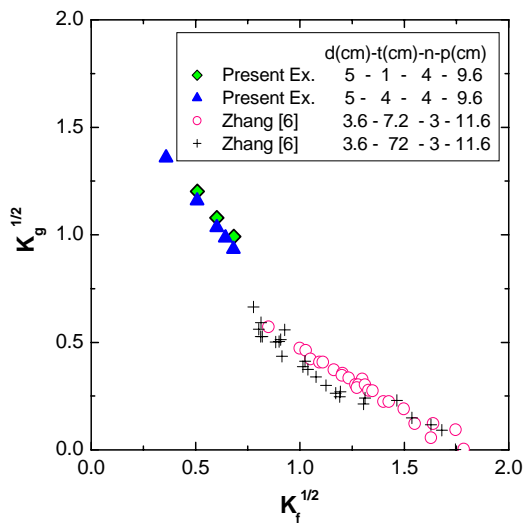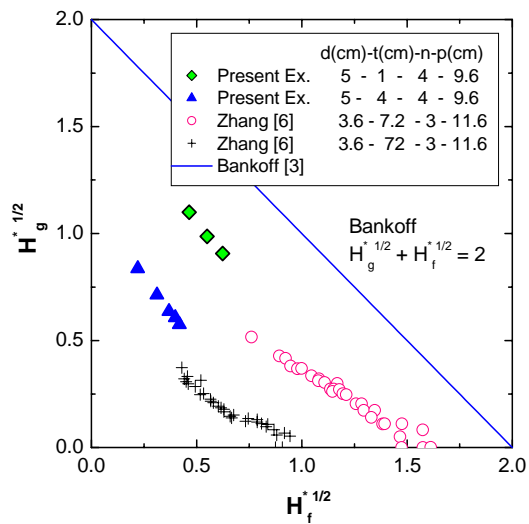

Fig. 8 CCFL data in j^* scaling

Fig. 9 CCFL data in K^* scaling

Fig. 10 CCFL data in H^* scaling